FULLY-DIFFERENTIAL POLY-SIC LAMÉ-MODE RESONATOR AND CHECKERBOARD FILTER

Sunil A. Bhave, Di Gao, Roya Maboudian, and Roger T. Howe
Berkeley Sensor & Actuator Center, 497 Cory Hall, University of California, Berkeley, CA 94720, USA

ABSTRACT

In this paper, we report the first fully-differential, electrostatically transduced RF MEMS resonator. The fully-differential electrode configuration not only cancels capacitive feedthrough between the drive and sense terminals but also eliminates the reduction in electromechanical quality factor (Q) from the large ohmic resistance of the polycrystalline silicon carbide (poly-SiC) suspension and anchor. Using this configuration, we have demonstrated a 173 MHz poly-SiC Lamé-mode resonator with a Q of 9,300 in air. By mechanically coupling five Lamé-mode resonators into a 2-D checkerboard, we have realized a 173 MHz center frequency band-pass filter with 110 kHz bandwidth and < 2 dB pass-band ripple.

1. INTRODUCTION

MEMS resonators are promising as micromechanical oscillators and filters in wireless communication systems because they have high quality factors and consume less power when compared to their discrete counterparts [1]. SiC has gained much attention as an attractive structural material in RF MEMS and NEMS applications due to its high acoustic velocity (15,400 m/s), Young's modulus (710 GPa) and extremely stable physiochemical properties [2]. Recently a single-ended electrostatically transduced SiC beam resonator was reported with a Q of 128 at 1.5 MHz [3]. The Q was two orders-of-magnitude lower than a similar electromagnetically transduced resonator (Q ~ 11,000 at 174.6 MHz) [4] because the 5 MΩ resistance of the resonator suspension and anchor degraded the measured Q of the electromechanical resonance. The Q of the electromagnetically transduced resonator was not affected by the ohmic resistance of the SiC suspension due to a thin layer of aluminum on top of the resonator.

The fully-differential electrode configuration presented in this paper minimizes such electrical dissipative losses and enables us to approach the high mechanical Q of a poly-SiC Lamé-mode resonator [5]. By fully-differential, we mean there are two electrodes for differential actuation and two electrodes for differential sensing of the resonator motion. This configuration offers several advantages including: (1) reduced capacitive feedthrough between drive and sense electrodes; (2) reduced ohmic losses in the resonator suspension and anchor thereby increased Q and (3) extended linearity for increased dynamic range and power handling.

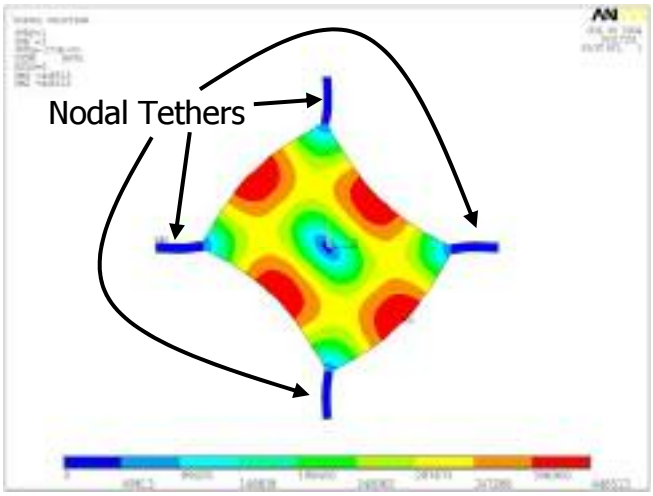

Figure 1: Isochoric (volume conserving) Lamé-mode shape simulated by ANSYS.

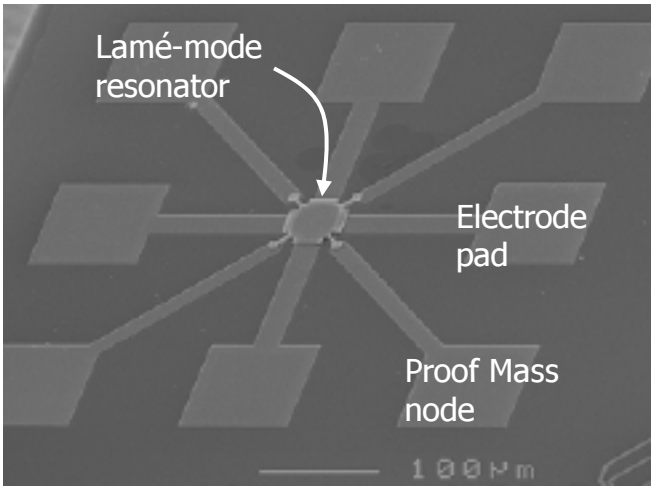

Figure 2: SEM of pad configuration of the poly-SiC Lamé-mode resonator.

2. POLY-SIC LAMÉ-MODE RESONATOR

Figure 1 presents the Lamé-mode shape of a square plate simulated in ANSYS. The resonator is anchored at the four nodal tethers to suppress energy loss through the anchors. Furthermore, the Lamé-mode shape is isochoric which minimizes energy loss due to thermoelastic dissipation (TED). The poly-SiC film used to fabricate the resonator (Figure 2) has a columnar grain microstructure with a strong <111> fiber texture, which means the Young's modulus, and Poisson's ratio of the film are independent of the

0-7803-8732-5/05/$20.00 © 2005 IEEE.

azimuthal angle in the vibration plane. In other words, the film can be considered to have isotropic mechanical properties in the vibration plane. In this case, the resonant frequency of vibration is given by [5]

$$f = \frac{1}{\sqrt{2} \cdot L} \sqrt{\frac{G}{\rho}} \qquad (1)$$

where L is the edge length of the square resonator, G is the shear modulus and ρ is the density of the poly-SiC film.

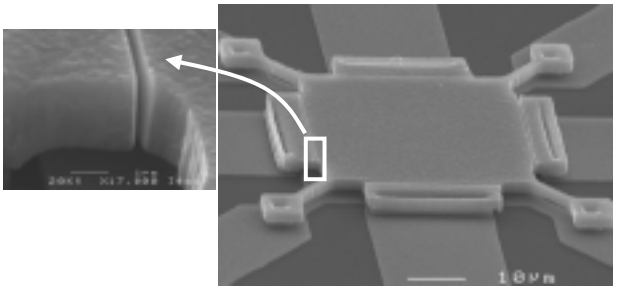

Figure 3: Poly-SiC Lamé-mode resonator with 195 nm FIB-cut electrostatic transducer gaps.

We have integrated the LPCVD and dry etching process for SiC [2] with conventional surface micromachining to form a poly-SiC RF MEMS process module. The process is similar to the multi-user MEMS process (MUMPs) except that the structural layer is poly-SiC instead of polysilicon. The photolithography steps after poly-SiC are performed at die-level due to limitation in prototype CVD reactor size. Therefore it is difficult to adapt the self-aligned, sub-micron spacer oxide process [6] for SiC. Instead have we used focused ion beam (FIB) to cut 195nm gaps through 2μm thick poly-SiC film (Figure 3).

3. EXPERIMENTAL RESULTS

In a typical two-port electrostatically transduced MEMS resonator, a DC polarization voltage is applied to the resonator proof-mass. However, in the case of FIB-cut electrostatic transducer gaps, the air-gap size is not uniform. Therefore we have used bias-Ts to apply an independent bias voltage at each drive and sense electrode and ground the proof-mass. During measurements, each DC supply is adjusted carefully in order to compensate for small differences in the air-gap sizes at different electrode locations. All measurements were performed using four bias-Ts from MiniCircuits Inc., a Cascade Microtech Inc. microwave probe station and coplanar shielded probes and semi-rigid SMA cables.

Single-ended drive, single-ended sense

Single-ended, two-port configuration for an electrostatically transduced polysilicon resonator limits the feedthrough capacitance between the drive and sense terminals to fringing-field capacitance above the resonator and through the substrate. Polysilicon resonators from audio frequency comb-drive resonators to wine-glass-mode disk resonators [7] are characterized using this configuration. However, poly-SiC has a sheet resistance of 900Ω/□ and contact resistance of 140 kΩ per square micron. Also the electrical resistance (R_{ohmic}) of the Lamé-mode resonator tethers and anchor was measured to be ~ 180 kΩ.

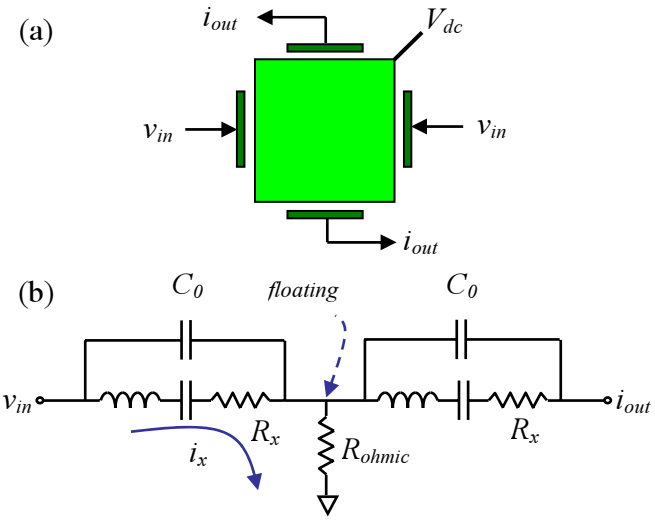

Figure 4: (a) Single-ended, two-port electrode configuration and (b) equivalent electrical model. When ohmic resistance of the suspension and anchor (R_{ohmic}) is larger than the motional impedance R_x, the proof-mass node is not a virtual ground. The feedthrough capacitance becomes $C_0/2$, instead of just the fringe capacitance.

Figure 4 shows the electrical model of the two-port configuration [8] in the presence of a resistive suspension and anchor. When the proof-mass node is resistive or it is not properly grounded, the feedthrough capacitance is $C_0/2$, and the ohmic resistance of the suspension and anchor (R_{ohmic} ~ 200 kΩ) is in series with the motional impedance (R_x ~ 18 kΩ), thereby increasing the dissipative losses in the resonator by over 10×. Hence, the measured transmission spectrum shows a high capacitive feedthrough floor and a resonance peak of < 1dB, which is insufficient to measure the Q of the resonator.

Single-ended drive, differential sense

Balanced electronic detection using dummy resonators has been demonstrated as an effective method for nulling capacitive feedthrough [4, 9]. This technique requires an identical resonator to be fabricated next to the resonator being characterized. A double-ended tuning fork with differential sense was recently demonstrated [10]; however, the differential configuration only excited the low Q swinging mode of the tuning fork.

The neighboring edges of the Lamé-mode resonator vibrate 180° out-of-phase. This has enabled us to easily implement differential sense configuration using a power

combiner and reduce the capacitive feedthrough (Figure 5(a), (b)). The fourth electrode, which was not used in the measurement, was grounded. The capacitive feedthrough nulling reduced the transmission floor to -67 dB making it possible to measure a Q of 1,050 at 173 MHz (Figure 5(c)). However, as shown in the electrical model the motional current passes through the ohmic resistance of the suspension and anchor and degrades the resonator Q.

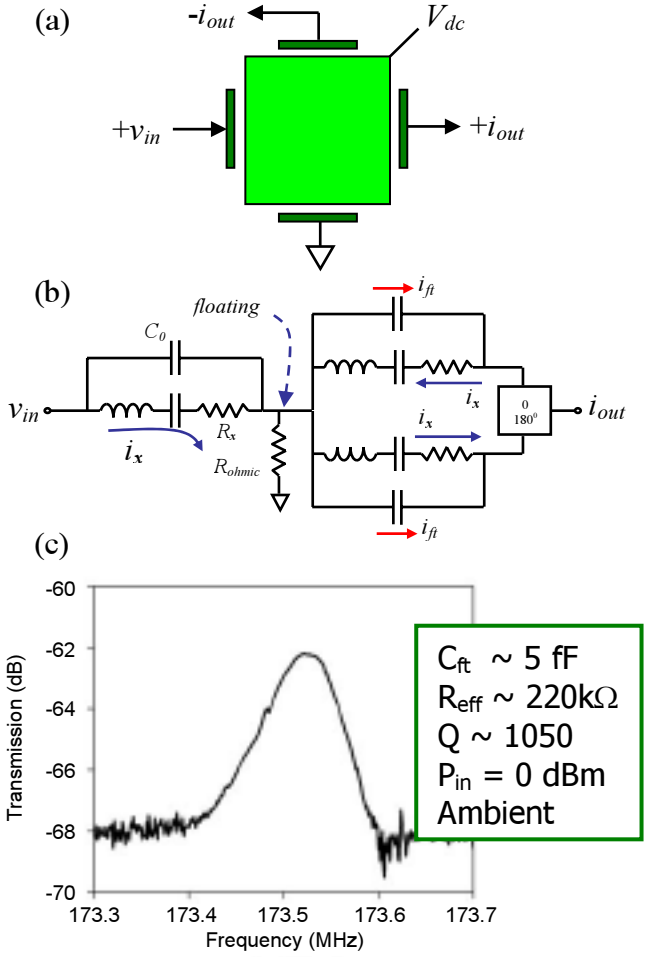

Figure 5: (a) Single-ended drive, differential sense electrode configuration, (b) equivalent circuit model and (c) transmission measurement with electromechanical Q of 1,050.

Differential drive, differential sense

The fully-differential configuration was implemented using two power-combiners (Figure 6(a), (b)). In this setup, the motional and feedthrough currents are nulled at the proof-mass node creating a virtual ground. Thus, no charge passes through the resonator suspension and anchor enabling us measure the high mechanical Q of 9,300 in air (Figure 6(c)).

The fully-differential configuration also cancels the second harmonic distortion term (HD2) thereby improving the power-handling capability and dynamic range of the resonator.

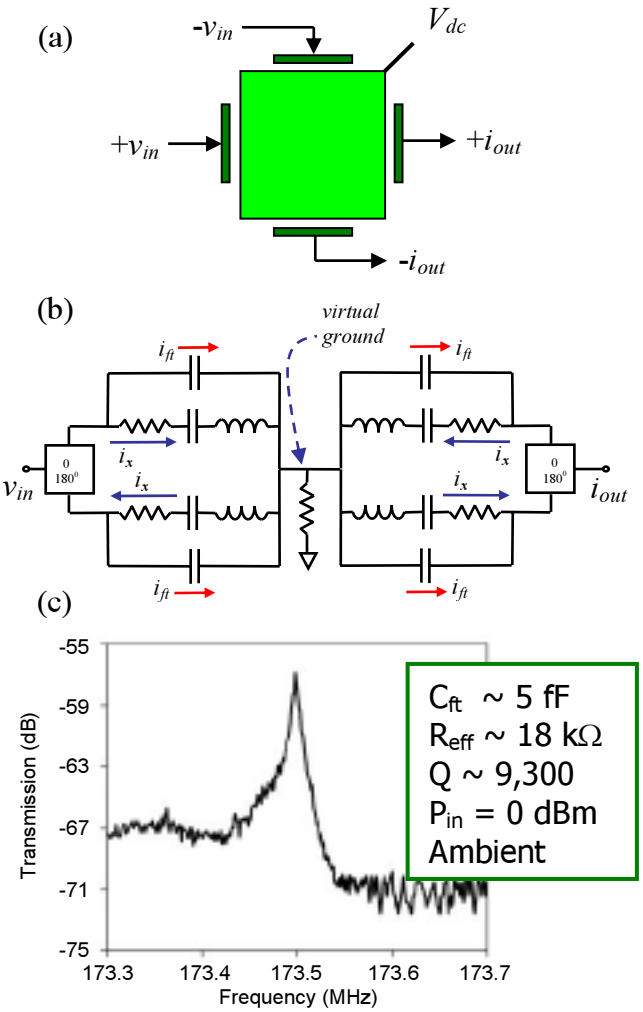

Figure 6: (a) Fully-differential electrode configuration and (b) equivalent circuit model using two power combiners. The motional and feedthrough currents add up at the proof-mass node ensuring there is no current flowing through the suspension and anchor. This eliminated the ohmic resistance and enabled us to measure a Q of 9,300 in air (c).

4. LAMÉ-MODE CHECKERBOARD FILTER

It is challenging to design mechanically coupled band-pass filters above 100 MHz because it is difficult to access the low-velocity coupling nodes of dilation-mode disk resonators [11]. However, Lamé-mode resonators have four nodal points along the perimeter which can be coupled together in a 2-D array.

The 2-D coupled checkerboard array (Figure 7(a)) adds two additional poles to the transmission pass-band (compared to a 1-D diagonally coupled array), and attenuates the ripple in the filter pass-band. Figure 7(b) shows the harmonic analysis (without modal damping) of the checkerboard filter. Figure 7(c) shows the measured transmission spectrum of the fully-differential checkerboard filter at 173 MHz center frequency with 110 kHz bandwidth, < 2 dB pass-band ripple and 12 dB stop-band rejection.

(a)

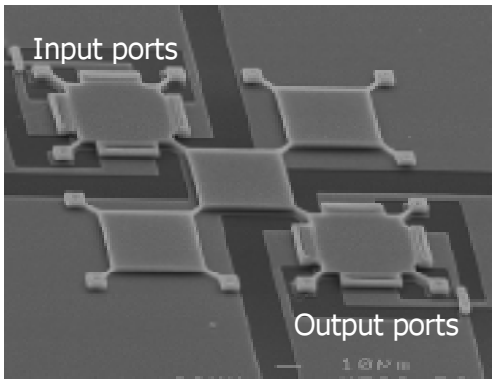

(b)

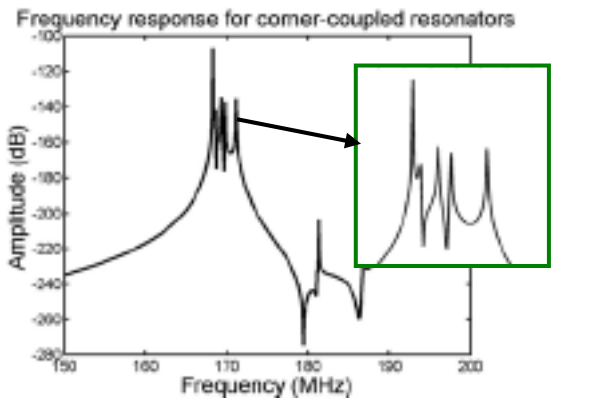

(c)

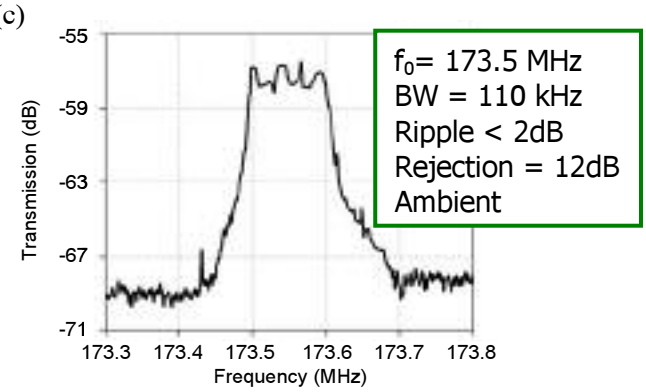

Figure 7: (a) SEM of 2-D checkerboard array filter (b) Bode plot of the checkerboard filter using FEAP and (c) measured differential transmission response in ambient. This measurement is an unmatched transmission measurement because the motional impedance is too large to perform impedance transforms and matching.

5. CONCLUSIONS

Although poly-SiC has high electrical resistance, it is an attractive material for RF MEMS resonators. We have demonstrated a fully-differential poly-SiC Lamé-mode resonator with a *Q* of 9,300 at 173 MHz in ambient. As we approach GHz frequencies and fabricate large resonator arrays and ring resonators, the sheet resistance of even polysilicon will present a bottleneck to scalability. The fully-differential technique confines the motional current to the periphery of the resonator body, preventing its flow through the resistive suspension, contacts, and interconnect. By mechanically coupling five Lamé-mode resonators into a 2-D checkerboard array we have realized a 173 MHz center frequency band-pass filter with 110 kHz bandwidth and <2dB pass-band ripple.

6. ACKNOWLEDGMENTS

This research was funded by DARPA NMASP program under grant# N66001-00-1-8955. We would like to thank David Bindel for FEA simulation of the checkerboard filter.

7. REFERENCES

[1] C. T.-C. Nguyen, "High-Q micromechanical oscillators and filters for communications", *IEEE International Symposium on Circuits and System*, Hong Kong (1997), pp. 2825-2828.

[2] D. Gao, B. J. Wijesundra, C. Carraro, C. W. Low, R. T. Howe, and R. Maboudian, "High modular polycrystalline 3C-SiC technology for RF MEMS", *Transducers 2003*, Boston, Massachusetts, June 8-12, 2003, pp. 1160-1163.

[3] R. Wiser, C. A. Zorman, and M. Mehregany, "Fabrication and testing of vertically-actuated polycrystalline silicon carbide micromechanical resonators for MHz frequency applications", *Transducers 2003*, Boston, Massachusetts, June 8-12, 2003, pp. 1164-1167.

[4] X. M. H. Huang, M. K. Prakash, C. A. Zorman, M. Mehregany, and M. L. Roukes, "Free-free beam silicon carbide nanomechanical resonators", *Transducers 2003*, Boston, Massachusetts, June 8-12, 2003, pp. 342-343.

[5] H. Majjad, J. -R. Coudevylle, S. Basrour, and M. Labachelerie, "Modeling and characterization of Lamé-mode microresonators realized by UV-LIGA", *Transducers 2001*, Munich, Germany, June 10-14, 2001, pp. 300-303.

[6] J. Wang, Z. Ren, and C. T.-C. Nguyen, "Self-aligned 1.14-GHz vibrating radial-mode disk resonators", *Transducers 2003*, Boston, Massachusetts, June 8-12, 2003, pp. 947-950.

[7] M. A. Abdelmoneum, M. U. Demirci, and C. T.-C. Nguyen, "Stemless wine-glass-mode disk micromechanical resonators", *MEMS 2003*, Kyoto, Japan, January 19-23, 2003, pp. 698-701.

[8] C.T.-C. Nguyen, "Micromechanical Signal Processors", *Ph.D. Thesis*, University of California, Berkeley, 1994.

[9] P. Rantakari, J. Kiihamaki, M. Koskenvuori, T. Lamminmaki, and I. Tittonen, "Reducing the effect of parasitic capacitance on MEMS measurements", *Transducers 2001*, Munich, Germany, June 10-14, 2001, pp. 1156-1159.

[10] E. P. Quévy, S. A. Bhave, H. Takeuchi, T.-J. King, and R. T. Howe, "Poly-SiGe high frequency resonators based on lithographic definition of nano-gap lateral transducers," *Hilton Head 2004*, Hilton Head Island, South Carolina, June 6-10, 2004, pp. 360-363.

[11] J. R. Clark, "Micromechanical disk resonators for wireless communications", *Ph.D. Thesis*, University of Michigan, 2003, pp. 89-110.